International Journal of Terrestrial Heat Flow and Applied Geothermics
VOL. 5, NO. 1 (2022); P. 45-50.
ISSN: 2595-4180
DOI: https://doi.org/10.31214/ijthfa.v5i1.84
IJTHFA
http://ijthfa.com/

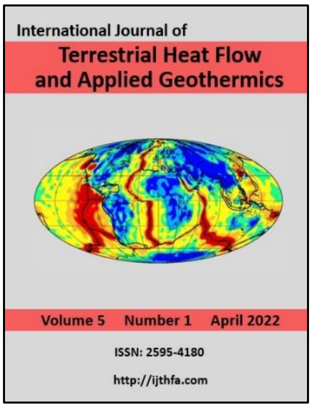

The Evaluation of the Thermal Field under Urban Heat Island Based on Borehole Temperature Measurements (Evidence from Yekaterinburg, Russia)

Dmitry Yu. Demezhko[1], Anastasiia A. Gornostaeva[1], Bogdan D. Khatskevich[1]

[1] Institute of Geophysics UB RAS, Yekaterinburg, Russia

Email address
ddem54@inbox.ru (D.Yu. Demezhko)
Corresponding author

Keywords
Urban heat island,
Borehole,
Underground temperatures,
Heat flux,
Heat content.

Received: January 25, 2022

Accepted: February 10, 2022

Published: April 02, 2022

Abstract

The paper deals with the analysis of the subsurface urban thermal field using temperature logging in boreholes. The method for the separation and quantification of temperature anomalies in an urban subsurface induced by climate change and the building construction at the local area has been described. The differences in the penetration dynamics for climate and local anomalies afford to estimate their contributions separately. The study was carried out by the example of the borehole IGF-280 located in Yekaterinburg, Russia. It was found that the value of local temperature anomaly caused by the building construction is much higher than that induced by climate change (11 K versus 1.4 K). But the climate temperature anomaly penetrates deeper than the local one (140 m for the climate anomaly versus 90 m for the local one). We also assessed changes in heat content due to climatic changes and building operation. The heat content of the rocks increased by $15.6 \cdot 10^7$ J/m^2 due to climate change over the past 150 years. The building input to the heat content increase is more than twice as higher – $38.6 \cdot 10^7$ J/m^2. About 40% of the heat content gain caused by climate change is concentrated in the 20-meter layer of rocks, and 97% of that – in the upper 100 m. 74% of the heat content gain due to the building influence are concentrated in the upper 20 m.

1. Introduction

An urban heat island effect is one of the major problems of modern climatology, ecology, and urban planning. Active modification of ground surface due to urbanization leads to changes in radiation balance of urban territory and, hence, to temperature increase of the urban environment in comparison with the rural area (Fergusson and Woodbury, 2007; Menberg et al., 2013; Esau et al., 2018). Since the discovery of this phenomenon two centuries ago by Luke Howard (Howard, 1818; Mills, 2008), this problem has only been escalating, and attention to the issue has been increasing. Most of studies have been focused on the investigation of the atmosphere, e.g., the features of its thermal, wind and humidity conditions, as well as the harmful substances distribution, while the method being meteorological observations (Oke, 1973; Rizwan et al., 2008; Lokoshchenko and Korneva, 2015; Dudorova and Belan, 2016; Brusova et al., 2017 etc.). However, increasing temperatures due to anthropogenic alterations in urban areas can be found not only in the atmosphere but also in the subsurface (Fergusson and Woodbury, 2007; Epting et al., 2013; Benz et al., 2015 and references therein). Changes in rock's temperature influence its filtration and strength properties (Liu et al., 2011). The heat entering the subsurface can be accumulated by groundwater and be spread laterally and vertically (Menberg et al., 2013). An underground thermal field contains the information on the heat flows integrated over sufficient long-time intervals. Therefore, its analysis allows the more precise evaluating of heat exchange at the ground surface in comparison with meteorological data.

Rock temperature at any depth is the sum of the steady-state component of thermal field produced by the heat flow from the Earth's interior and transient temperature anomaly caused by the ground surface temperature (GST) variations. The seasonal temperature waves disappear at the depth of 15–25 m. The influence of long-term climate change is observed up to hundreds of meters in case of millennial climate variations and even to 1-2 kilometers for the glacial—interglacial cycles (Pollack et al., 1993; Pollack and Huang, 2000; Demezhko and Shchapov, 2001; Bodri and Cermak, 2007; Huang et al., 2009). In case of urban heat islands local transformations of ground surface including building construction, alterations of surface cover, an urban infrastructure development, etc., contribute significantly to transient temperature anomaly of an urban subsurface in addition to climate change forcing (Taniguchi et al., 2005, 2007; Dedecek et al., 2012; Menberg et al., 2013).

The main source of information on the subsurface temperatures inside the city is shallow boreholes (Ferguson and Woodbury, 2007; Huang et al., 2009; Dedecek et al., 2012). Temperature logging provides estimating the modern thermal regime of the subsurface. In this paper, we describe how to separate and quantify the subsurface temperature anomalies caused by climate change and the heated building at the local area by the analysis of temperature log using the example of the borehole located in Yekaterinburg.

2. Materials and methods

The borehole IGF-280 was drilled in 1983 in Yekaterinburg in the territory of the Institute of Geophysics UB RAS. The borehole is cased with a 79 mm inner diameter steel pipe to a depth of 44 m, and there is an open hole with a diameter of 76 mm below (to a depth of 202 m) and 59 mm (to the bottom at a depth of 280 m). At the interval of 0 – 20 m, the borehole penetrates the weathering crust of gabbro, below – dense gabbro with rare peridotite, amphibolite, quartz inclusions. In 1984, a heated production building without a basement 30 X 60 m in size was built in the borehole site. The borehole is located in the eastern corner of the building at a distance of 5 and 10 m from the walls (see Figures 1, 3).

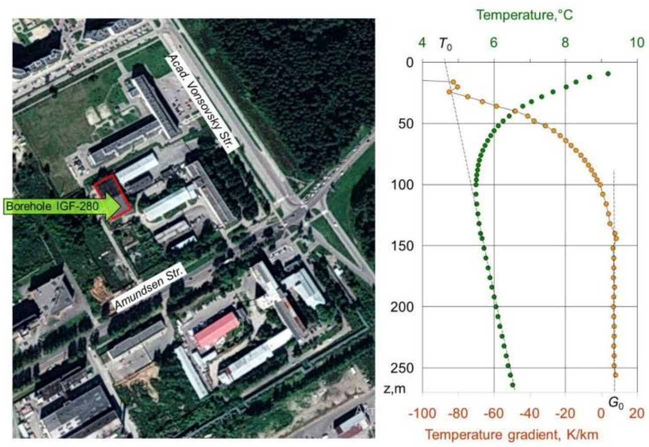

Figure 1 - Borehole location (left) and the temperature-depth profile measured in the IGF-280 borehole (right).

A precision discrete temperature measurement using a quartz thermometer was carried out in January 2020 (Figure 1). The temperature-depth profile is determined by two factors, i.e., climate changes in Yekaterinburg and the increase in temperature at the local area of the heated building. It can be represented as follows:

$$T(z,t) = T_0 + G_0 z + \Delta T^{clim}(z,t) + \Delta T^{loc}(z,t) \quad (1),$$

where T_0 is an initial undisturbed ground surface temperature (GST); z is the depth; t is time; G_0 is the geothermal gradient; $\Delta T^{clim}(z, t)$ and $\Delta T^{loc}(z, t)$ are the temperature anomalies related to changes in urban climate and the local temperature changes in the building, respectively. For the borehole IGF-280 T_0 = 4.67 °C, $G_0 = 6.9 \cdot 10^{-3}$ K/m (see Figure 1).

Figure 2 shows the history of surface air temperature (SAT) variations in Yekaterinburg almost two centuries long (http://pogodaiklimat.ru/history/28440.htm). We suppose that even if GST during this period was slightly higher than SAT, it varied synchronously with SAT at the same amplitude. This assumption was confirmed by a direct comparison of geothermal reconstructions and instrumental data (Demezhko and Golovanova, 2007), by the numerical simulation results (Gonzales-Rouco et al., 2003, 2006), and by the data of temperature monitoring in boreholes (Chapman et al., 2004). To simulate the thermal field due to changing climate, the initial SAT history until 1984 (before the building construction) was approximated by a series of steps of individual intervals of constant temperature (Figure 2, bold blue curve). The mean SAT until 1900 is equal to 0.59 °C that is lower than undisturbed GST estimated from the temperature-depth profile by 4.1 °C (T_0 = 4.67 °C). Thus, climatic GST history is equal to SAT shifted by 4.1 °C. After 1984 urban climate did not influence the subsurface thermal field, therefore, the GST was considered constant.

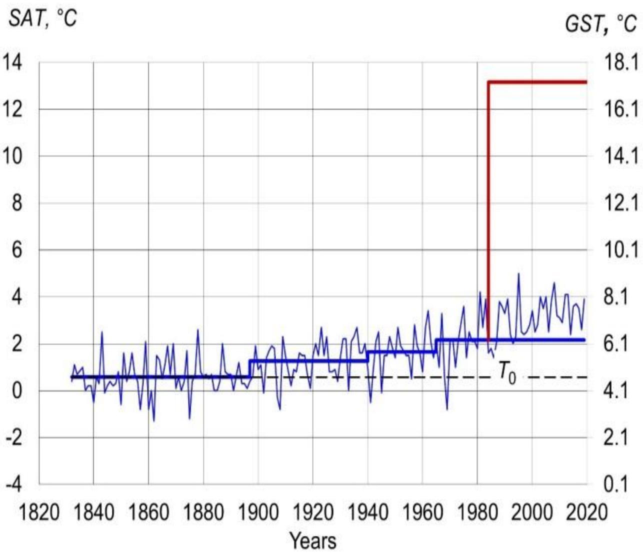

Figure 2 - Mean annual SAT in Yekaterinburg according to meteorological data (thin blue curve) and the approximation of the GST variation before (bold blue curve) and after (red curve) the building construction.

For the GST history approximated by a series of steps of individual intervals with constant temperature, the vertical distribution of temperature anomaly for the source-free laterally homogeneous semi-infinite medium without any features of hydrological activity can be expressed as a solution of a 1-D non-stationary heat conduction equation (Carslaw and Jaeger, 1958):

$$\Delta T^{clim}(z,t) = \sum_{i=1}^{n} D_i^{clim} erfc\frac{z}{L}, L = 2\sqrt{at_i} \quad (2),$$

where D_i^{clim} is the amplitude of the i-th stepwise change of GST; t_i is time elapsed after that to the moment of temperature logging (the present); z is the depth; a is the thermal diffusivity; *erfcU* is the complementary error function.

Temperature anomaly induced by the building construction

In contrast to the climate impact, the influence of a building spreads to a limited surface area. The propagation rate of the local temperature anomaly differs from those of anomaly caused by climate change. For the circle anomalous zone of radius r, an analytic expression for the vertical distribution of temperature anomaly in the center of a circle was obtained in (Demezhko and Ryvkin, 1996; Demezhko, 2001):

$$\Delta T^{loc}(z,t,r) = D^{loc}\left[erfc\left(\frac{z}{L}\right) - \frac{z}{\sqrt{z^2+r^2}}erfc\left(\frac{\sqrt{z^2+r^2}}{L}\right)\right], L = 2\sqrt{at} \quad (3)$$

where D^{loc} is the amplitude of a stepwise increase in local GST.

However, the analyzed borehole is located under a noncircular building that does not allow using the expression (3) for a circle directly. To calculate the local temperature anomaly induced by the source of arbitrary shape, one can use the circular sectors approximation method (Balobaev et al., 2008). Pattern and outline of the circular sectors approximating the building over the IGF-280 are shown in Figure 3 and in Table 1. The vertical distribution of temperature anomaly can be calculated as a sum of contributions of all sectors:

$$\Delta T^{loc}(z,t) = \sum_{i=1}^{n} \Delta T_i^{loc}(z,t,r_i)\frac{\phi_i}{2\pi} \quad (4),$$

where r_i and φ_i are the radius and the angle at center of i-th sector, respectively.

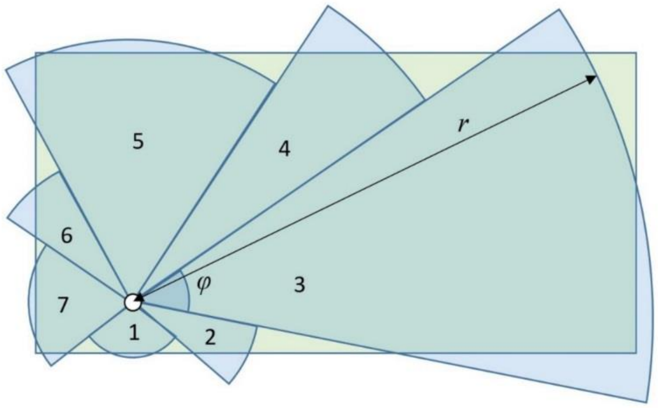

Figure 3 - Outline of the circular sectors approximating the building over the IGF-280.

Table 1 - Pattern of the building and the approximating circular sectors (The building: length – 61 m, width – 30 m. The borehole IGF-280: the distance from the nearest walls – 10 and 5 m)

Approximating sectors							
Sector's number, i	1	2	3	4	5	6	7
φ, degrees	103	28	44	23	62	28	72
r, m	5	15	52	36	27	15	11

To calculate temperature anomaly by equations (2 – 4), we know the chronology and amplitude of climate change from the instrumental data, as well as the date of the building construction, i.e., 36 years ago. Two parameters are not determined, i.e., the thermal diffusivity of rocks a, and the amplitude of a stepwise GST increase D^{loc}. Thermal diffusivity controls the propagation rate of temperature anomaly and consequently the depth of the anomaly penetration. According to the data by Robertson (1988), the value of thermal diffusivity of gabbro lies between $(0.9 – 1.1)\cdot10^{-6}$ m^2/s, however, *in situ* it might differs from these estimates. D^{loc} controls the amplitude of temperature anomaly. These two parameters have different effects on the form of temperature anomaly. Hence, one can estimate a and D^{loc}, as well as the values of temperature anomalies due to urban climate and the building individually calculating the minimum of the residual error:

$$R(a, D^{loc}) = \sqrt{\frac{\sum_{i=1}^{n}\left[\Delta T_i^{clim}(z_i,a)+\Delta T_i^{loc}(z_i,a,D^{\text{лок}})-\Delta T_i^{meas}(z_i)\right]^2}{n-1}} \rightarrow min \quad (5)$$

3. Results

Transient climate and local temperature anomalies

The residual (5) was calculated for each point of the temperature log except for two upper points. It seems that these two points are located within the limits of annual heat exchange. The minimal value of the residual error R_{min} = 0.032 K is achieved at $a = 0.9\cdot10^{-6}$ m^2/s and D^{loc} = 11 K (see Figure 4). The surface R (a; D^{loc}) has an elongated minimum, therefore, within the isoline R = 0.05 K, the parameters (a; D^{loc}) can vary from (0.8; 12.0) to (1.0; 9.3).

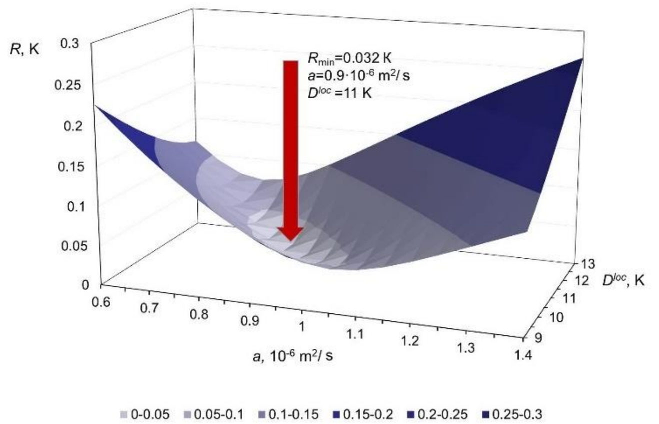

Figure 4 - The residual error surface

Temperature anomalies induced by the variations in GST due to urban climate and the local influence of the building, corresponding to the minimal value of the residual error are shown in Figure 5. The anomaly due to climate change has a maximal value of 1.4 K at the surface and decays to 0.1 K at a depth of 140 m. The local temperature anomaly has a maximal value of 11 K at the surface and decays to the value of 0.1 K at a depth of 90 m. The modeling has shown that the local anomaly became stationary already about 10 years ago, and its penetration to the depth was terminated.

Changes in the heat content

Climate change in Yekaterinburg and the building construction over the borehole IGF-280 led to changes in the heat content. A total change of the heat content Q (z_1, z_2) in a layer limited by depths z_1, z_2 can be directly estimated from a measured temperature anomaly.

$$Q(z_1, z_2) = \rho C \int_{z_1}^{z_2} \Delta T(z) dz \quad (6).$$

Here ρ and C are the density and the specific heat capacity of rocks (gabbro). The contributions of climate and the building in a total change of the heat content can be estimated by the modeled temperature anomalies that describe the measured anomaly adequately. For gabbro ρ = 2980 kg/m^3, C = 720 J/(kg K) (Robertson, 1988).

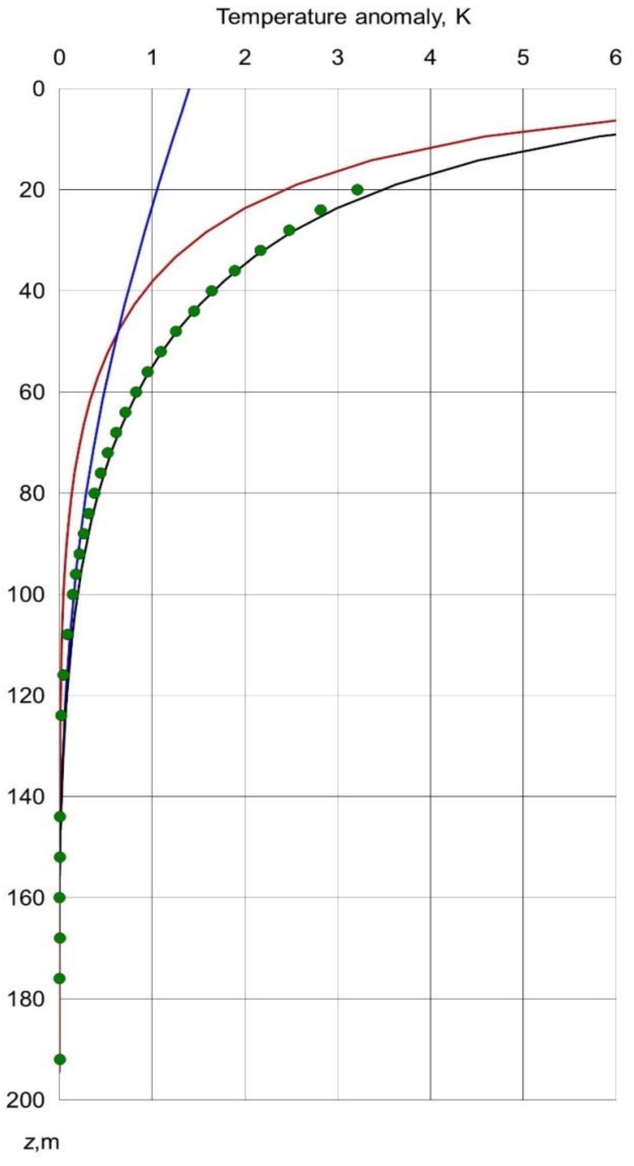

Figure 5 - Temperature anomalies in the IGF-280 borehole: measured ΔT^{meas} (green points), anomaly due to climate change ΔT^{clim} (blue curve), local influence of the building ΔT^{loc} (red curve), and cumulative effect ΔT^{sum} (black curve).

The heat content of the rocks increased by 15.6·10^7 J/m^2 due to climate variation (see Table 2). This estimate is slightly higher than the average for the Urals, i.e., 12.9·10^7 J/m^2 (Demezhko and Gornostaeva, 2015a) obtained using another approach, i.e., from the reconstructed surface heat flux history (Demezhko and Gornostaeva, 2015b). The building input to the heat content increase is more than twice as higher – 38.6·10^7 J/m^2.

Table 2 - Change in the heat content at different intervals of the borehole IGF-280, x10^7 J/m^2.

Interval, m	Climate contribution	Building contribution	Total
0 – 20	6.3	28.7	35.0
20 – 100	8.8	9.8	18.5
100 – 200	0.5	0.2	0.7
0 – 200	15.6	38.6	54.2

About 40% of the heat content gain caused by climate change is concentrated in the 20-meter layer of rocks, and 97% of that – in the upper 100 m. 74% of the heat content gain due to the building influence are concentrated in the upper 20 m. An average heat flux into the subsurface during the building's usage period was equal to 0.34 W/m^2. For comparison, in Karlsrohe the anthropogenic heat flux from buildings to the subsurface was equal to 3.61 ± 3.37 W/m^2, in Köln it was 0.57 ± 0.47 W/m^2 (Benz et al., 2015). In Basel Epting et al. (2013) estimated heat fluxes from different buildings in the range of 0.18 to 16 W/m^2. In our case, a heating system of the building over 36 years of operation has produced 4.3·10^{11} J/m^2 of heat. Only a small part of this energy has spent to the heat content gain, i.e., 38.6·10^7 J/m^2 (0.09%). An even lower value is given in studies of nearly a century of work of a brick factory in Stewartby, UK (Westaway et al., 2015). The heat stored in the interior under the factory was only equal to 0.03% of the energy released by burning fuel.

4. Conclusions

The study has shown that the present subsurface thermal field observed in Yekaterinburg by the precise temperature logging carried out in the IGF-280 borehole is strongly influenced both by the recent urban climatic change and by the local anthropogenic forcing from the heated building construction. It was possible to separate the transient signals of the two sources and to evaluate their contributions into subsurface thermal field individually using the differences in the penetration dynamics for climate and local anomalies.

It was found that the value of local temperature anomaly caused by the building construction is much higher than that induced by climate change (11 K versus 1.4 K). But the climate temperature anomaly penetrates deeper than the local one (140 m for the climate anomaly versus 90 m for the local one). The local anomaly can be associated not only with the forcing from a building but also with changes of heat transfer conditions at the ground surface. Depending on the surface covering material (e.g., grass, gravel, asphalt, concrete etc.), the difference in maximal values may reach 10 – 20 K for diurnal temperatures and up to several degrees for mean annual temperatures (Santamouris, 2013 and references herein), that is comparable to the building influence.

The building input to the heat content increase is more than twice as higher than the climate one (38.6·10^7 versus 15.6·10^7 J/m^2). About 40% of the heat content gain caused by climate change is concentrated in the 20-meter layer of rocks, and 97% of that – in the upper 100 m. 74% of the heat content gain due to the building influence are concentrated in the upper 20 m. An additional underground heat accumulated under the urban heat island can be treated not only as a factor of a heat pollution but also as a renewable energy source for heat pumps. The developed approach allows evaluating the potential of such energy source.

5. Acknowledgments

Revision of this text benefited from comments by the editorial board of JTHFA.

References

Balobaev, V.T., Kutasov, I.M., Eppelbaum, L.W. 2008. Borehole paleoclimatology – the effect of deep lakes and "heat islands" on temperature profiles. Climate of the Past Discussions 4, 415–432. DOI: 10.5194/cpd-4-415-2008.

Benz, S.A., Bayer, P., Menberg, K., Jung, S., Blum, P. 2015. Spatial resolution of anthropogenic heat fluxes into urban aquifers. Science of The Total Environment 524–525, 427–439. DOI: 10.1016/j.scitotenv.2015.04.003.

Bodri, L., Cermak, V. 2007. Borehole climatology: a new method how to reconstruct climate. Elsevier, 352 p.

Brusova, N.E., Kuznetsova, I.N., Nahaev, M.I. 2017. Thermal disturbance in the megapolis on the background of the regional surface air temperature variability. Proceedings of the Hydromet center of Russia 365, 22–34 (in Russian with English summary). DOI: 10.15372/AOO20160510.

Carslaw, H.., Jaeger, J.C. 1958. Conduction of heat in soils. Clarendon Press, Oxford, 510 p.

Chapman, D.S., Bartlett, M.G., Harris, R.N. 2004. Comment on “Ground vs. surface air temperature trends: Implications for borehole surface temperature reconstructions” by M.E. Mann and G. Schidt. Geoph. Res. Lett. 31, L07205. DOI: 10.1029/2003GL019054.

Dědeček, P., Šafanda, J., Rajver, D. 2012. Detection and quantification of local anthropogenic and regional climatic transient signals in temperature logs from Czechia and Slovenia. Climatic Change 113 (3), 787 – 801. DOI 10.1007/s10584-011-0373-5.

Demezhko, D.Yu. 2001. Geothermal Method for Paleoclimate Reconstruction (Examples from the Urals, Russia). Russ. Acad. of Sci., Urals Branch, Ekaterinburg, 143 p. (in Russian).

Demezhko, D.Yu., Golovanova, I.V. 2007. Climatic changes in the Urals over the past millennium – an analysis of geothermal and meteorological data. Climate of the Past 3, 237 – 242. In: www.clim-past.net/3/237/2007/.

Demezhko, D.Yu., Gornostaeva, A.A. 2015a. Reconstruction of Ground Surface Heat Flux Variations in the Urals from Geothermal and Meteorological Data. Izvestiya Atmospheric and Oceanic Physics 51 (7), 723 – 736.

Demezhko, D.Y., Gornostaeva, A.A. 2015b. Late Pleistocene–Holocene ground surface heat flux changes reconstructed from borehole temperature data (the Urals, Russia). Climate of the Past 11, 647 – 652. DOI:10.5194/cp-11-647-2015.

Demezhko, D.Yu., Ryvkin, D.G. 1996. Consideration of local surface temperature anomalies in paleoclimatic interpretation of borehole thermometry data. Deponent VINITI 1411-B96 (in Russian).

Demezhko, D.Y., Shchapov, V.A. 2001. 80 000 years ground surface temperature history inferred from the temperature-depth log measured in the superdeep hole SG-4 (the Urals, Russia). Global and Planetary Change 29, 219 – 230.

Dudorova, N.V., Belan, B.D. 2016. Estimation of factors determining formation of the urban heat island in Tomsk. Atmospheric and Oceanic Optics 29 (5), 426 – 436 (in Russian with English summary).

Epting, J., Händel, F., Huggenberger, P. 2013. Thermal management of an unconsolidated shallow urban groundwater body. Hydrology and Earth system sciences 17, 1851 – 1869. DOI:10.5194/hess-17-1851-2013.

Esau, I., Miles, V. 2018. Exogenous drivers of surface urban heat island in Northern West Siberia. Geography Environment Sustainability 11 (3), 83 – 99. DOI: 10.24057/2071-9388-2018-11-3-83-99.

Ferguson, G., Woodbury, A.D. 2007. Urban heat island in the subsurface. Geophysical Research Letters 34 (23), L23713. DOI: 10.1029/2007GL032324.

Gonzales-Rouco, J.F., von Storch, H., Zorita, E. 2003. Deep soil temperature as proxy for surface air temperature in coupled model simulation of the last thousand years. Geophysical Research Letters 30 (21), 2116. DOI: 10.1029/2003GL018264.

Gonzales-Rouco, J.F., Beltrami, H., Zorita, E., von Storch, H. 2006. Simulation and inversion of borehole temperature profiles in surrogate climates: Spatial distribution and surface coupling. Geophysical Research Letters 33, L01703. DOI: 10.1029/2005GL024693.

Howard, L. 1818. The climate of London. W Phillips, sold also by J. and A. Arch 1, 221 p.

Huang, S., Taniguchi, M., Yamano, M., Wang, C. 2009. Detecting urbanization effects on surface and subsurface thermal environment — a case study of Osaka. Science of the Total Environment 407, 3142 – 3152. DOI: 10.1016/j.scitotenv.2008.04.019.

Liu, C., Shi, B., Tang, C., Gao, L. 2011. A numerical and field investigation of underground temperatures under Urban Heat Island. Building and Environment 46 (5), 1205 – 1210. DOI: 10.1016/j.buildenv.2010.12.015.

Lokoshchenko, M.A., Korneva, I.A. 2015. Underground urban heat island below Moscow city. Urban Climate 13, 1 – 13. DOI: 10.1016/j.uclim.2015.04.002.

Mills, G. 2008. Luke Howard and the climate of London. Weather 63 (6), 153 – 157. DOI: 10.1002/wea.195.

Menberg, K., Blum, P., Schaffitel, A., Bayer, P. 2013. Long-term evolution of anthropogenic heat fluxes into a subsurface urban heat island. Environmental science & technology 47 (17), 9747 – 9755. DOI: 10.1021/es401546u.

Oke, T.R. 1973. City size and the urban heat island. Atmospheric Environment 7 (8), 769 – 779.

Pollack, H., Hurter, S., Johnson, J. 1993. Heat-flow from the Earth’s interior — analysis of the global data set. Reviews of Geophysics 31 (3), 267 – 280.

Pollack, H.N., Huang, S. 2000. Climate reconstruction from subsurface temperatures. Annual Review of Earth and Planetary Sciences 28, 339 – 365.

Rizwan, A.M., Dennis, L.Y.C., Chunho, L.I.U. 2008. A review on the generation, determination and mitigation of Urban Heat Island. Journal of Environmental

Sciences 20 (1), 120 – 128. DOI: 10.1016/S1001-0742(08)60019-4.

Robertson, E.C. 1988. Thermal properties of rocks. Open-File Report 88-441, Reston, Virginia, 106. In: https://pubs.usgs.gov/of/1988/0441/report.pdf.

Santamouris, M. 2013. Using cool pavements as a mitigation strategy to fight urban heat island – A review of the actual developments. Renewable and Sustainable Energy Reviews 26, 224 – 240. DOI: 10.1016/j.rser.2013.05.047.

Taniguchi, M., Uemura, T., Sakura, Y. 2005. Effects of urbanization and groundwater flow on subsurface temperature in three megacities in Japan. Journal of Geophysics and Engineering 2, 320 – 325. DOI: 10.1088/1742-2132/2/4/S04.

Taniguchi, M., Uemura, T., Jago-on, K. 2007. Combined effects of urbanization and global warming on subsurface temperature in four Asian cities. Vadose Zone J 6 (3), 591 – 596. DOI:10.2136/vzj2006.0094.

Westaway, R., Scotney, P.M., Younger, P.L., Boyce, A.J. 2015. Subsurface absorption of anthropogenic warming of the land surface: The case of the world's largest brickworks (Stewartby, Bedfordshire, UK). Science of the Total Environment 508, 585 – 603. DOI: 10.1016/j.scitotenv.2014.09.1090048-9697.